Articles

Chimeragenesis of the Fatty Acid Binding Site of Cytochrome P450BM3. Replacement of Residues 73−84 with the Homologous Residues from the Insect Cytochrome P450 CYP4C7†

Marat B. Murataliev,*,‡ Long N. Trinh,‡ Lani V. Moser,‡ Robert B. Bates,‡ René Feyereisen,§ and F. Ann Walker‡

Department of Chemistry, University of Arizona, Tucson, Arizona 85721-0041, and INRA Centre de Recherches d'Antibes, 1382 Route de Biot, 06560 Valbonne, France

Received September 16, 2003; Revised Manuscript Received December 3, 2003

ABSTRACT: A protein fragment of P450BM3 (residues 73−84) which participates in palmitoleate binding was subjected to scanning chimeragenesis. Amino acids 73−84, 73−78, 75−80, and 78−82 were replaced with the homologous fragments of the insect terpenoid hydroxylase CYP4C7. The four chimeric proteins, C(73−84), C(73−78), C(75−80), and C(78−82), were expressed, purified, and characterized. All the chimeric proteins contained all the cofactors and catalyzed monooxygenation of palmitate and of the sesquiterpene farnesol. Chimeragenesis altered substrate binding as shown by the changes in the amplitude of the palmitate-induced type I spectral shift. C(78−82) had monooxygenase activities close to those of P450BM3, while the rest of the chimeric proteins had monooxygenase activities that were inhibited relative to that of wild-type P450BM3. The extent of inhibition of the chimeric proteins varied depending on the substrate, and in the case of C(73−84), farnesol and palmitate oxidation was inhibited by 1 and 4 orders of magnitude, respectively. ^{1}H NMR spectroscopy and GC−MS were used to identify products of farnesol and palmitate oxidation. Wild-type P450BM3 and all chimeric proteins catalyzed oxidation of farnesol with formation of 9-hydroxyfarnesol and farnesol 10,11- and 2,3-epoxides. Three of the four chimeric proteins also formed a new compound, 5-hydroxyfarnesol, which was the major product in the case of C(73−78). In addition to hydroxylation of the C13−C15 atoms, the chimeric enzymes catalyze significant hydroxylation of the C10−C12 atoms of palmitate. In the case of C(78−82), the rates of formation of 11- and 12-hydroxypalmitates increased 7-fold compared to that of wild-type P450BM3 to 106 and 212 min^{-1}, respectively, while the rate of 10-hydroxypalmitate synthesis increased from zero to 106 min^{-1}. Thus, chimeragenesis of the region of residues 73−84 of the substrate binding site shifted the regiospecificity of substrate oxidation toward the center of the farnesol and palmitate molecules.

Cytochromes P450 comprise a superfamily of enzymes (*1*) that metabolize a wide range of structurally diverse substrates and catalyze dozens of chemical reactions, many of which are of biotechnological interest (*2*−*4*). The diversity of substrates and reactions that are catalyzed attracts the attention of researchers to P450 proteins as potential templates for genetically engineering enzymes with new substrate specificity, regiospecificity, and/or stereospecificity of catalysis.

Cytochrome P450BM3[1] is a soluble fatty acid hydroxylase of *Bacillus megaterium* (*5*; see also reviews *6* and *7*). The single-polypeptide enzyme (M_r = 119 000) consists of two distinct domains, heme and flavoprotein, and contains all the cofactors, heme, FAD, and FMN, required for catalysis. P450BM3 catalyzes hydroxylation of fatty acids with rates 10^2−10^3 times higher than the rate of catalytic turnover of most eukaryotic P450 enzymes (*5*). Moreover, P450BM3 catalysis is tightly coupled: the stoichiometry of fatty acid hydroxylated to NADPH consumed is close to 1 under both steady state and single-turnover conditions (*8*−*10*). This highly efficient catalysis makes P450BM3 an ideal enzyme for use in biotechnology. However, due to relatively narrow substrate specificity and regiospecificity, potential biotechnological use of P450BM3 will require tailoring by genetic engineering (*11*).

Most of the previous attempts to alter the substrate specificity of P450BM3 dealt with mutagensis of individual

† This work was supported by National Institutes of Health Grant GM39014.

* To whom correspondence should be addressed: Department of Chemistry, P.O. Box 210041, University of Arizona, Tucson, AZ 85721-0041. Telephone: (520) 621-9697. Fax: (520) 626-9300. E-mail: mmuratal@u.arizona.edu.

‡ University of Arizona.

§ INRA Centre de Recherches d'Antibes.

[1] Abbreviations: BMP, individually expressed heme domain of P450BM3; CYP4C7, cytochrome P450 4C7; GC-FID, gas chromatography with flame ionization detection; GC−MS, gas chromatography and mass spectrometry; NMR, nuclear magnetic resonance; P450, cytochrome P450; P450BM3, cytochrome P450 CYP102 isolated from *Bacillus megaterium*; TMS, trimethylsilyl.

10.1021/bi035674b CCC: $27.50
Published on Web 01/29/2004

Table 1: Mutagenic Primers Used for Chimeragenesis of P450BM3

chimera	primer
C(73−84)	CTTAAGTTACGAGTACAGCTTTCTATTTCCCTGGCTGGGTACAGGGTTATTTACAAGCTGGACGC
C(73−78)	CTTAAGTTACGAGTACAGCTTTCTACGTGATTTTGCAGGAGACGGGTTATTTAC
C(75−80)	CTTAAGTCAAGCGTACAGCTTTCTATTTCCCTTTGCAGGAGACGGGTTATTTACAAGC
C(78−82)	CTTAAGTCAAGCGCTTAAATTTCTATTTCCCTGGCTGGGTGACGGGTTATTTACAAGCTGGACGC

amino acid residues or several residues located in different structural elements of the enzyme. Mutagenesis of a number of residues of the heme domain of P450BM3 altered the affinity for substrates, turnover rates, and regiospecificity of fatty acid hydroxylation (*12*−*17*). Directional or rational evolution has recently been applied to P450BM3 (*18*−*21*). In these studies, replacement of eight amino acids of the substrate access channel resulted in several enzyme variants with novel catalytic activities. A "molecular Lego" approach has also been applied, in which CYP2E1, starting from residue 81, was fused between the first 54 amino acids and reductase domains of P450BM3 (*22*). The resulting clones expressed protein with P450-like properties, but the catalytic function was not characterized.

The structures of the heme domain of P450BM3, also called BMP, with and without a bound fatty acid substrate, have been determined (*23*, *24*). The structure with palmitoleate bound revealed a number of protein fragments that form the substrate binding pocket and amino acid residues that contact the fatty acid (*24*). No systematic studies on the structure−function relationships of the protein fragments of the substrate binding pocket and/or of the catalytic site have been carried out. This warranted a detailed investigation into the role of the individual fragments of the catalytic site in determining the substrate and catalytic specificity of P450BM3. Here we report application of the "scanning chimeragenesis" approach in studying the roles of individual structural elements that determine the substrate specificity and in engineering enzyme variants with new catalytic activities. In this approach, amino acids 73−84 of the P450BM3 substrate binding site was replaced with the homologous fragment from another cytochrome P450 enzyme, CYP4C7.

CYP4C7, the insect enzyme catalyzing regio- and stereospecific hydroxylation of farnesol to produce (10*E*)-12-hydroxyfarnesol (*25*), was chosen for chimeragenesis of P450BM3. The choice was determined by the fact that P450BM3 also catalyzes oxidation of farnesol, but the two enzymes form different products. In this study, we replaced amino acid residues 73−84, 73−78, 75−80, and 78−82 of the P450BM3 substrate binding site with the corresponding fragments of CYP4C7. Four functional P450BM3−CYP4C7 chimeric proteins with altered substrate binding and catalytic properties were expressed, purified, and characterized. Reaction products with palmitate and farnesol were identified by GC−MS and ^{1}H NMR spectroscopy. Chimeragenesis shifted the regiospecificity of monooxygenation and resulted in the formation of new products not seen with wild-type P450BM3: 10-hydroxypalmitate and 5-hydroxyfarnesol.

EXPERIMENTAL PROCEDURES

Genetic Engineering of the Chimeric P450BM3 Proteins. PCR was carried out using the pbsBM3 vector (*26*) that harbors the coding sequence for P450BM3 as a template. Mutagenic primers used to introduce the CYP4C7-specific sequences are listed in Table 1, and Figure S1 of the Supporting Information shows the cloning scheme for P450BM3 chimeragenesis. The primers were designed to take advantage of the unique *Afl*II restriction site located upstream of the replacement fragment. This *Afl*II site was used for further cloning of the PCR products. A reverse primer (gct tca ccg cgg tca gcg) was used for all of the PCRs. Each DNA amplification reaction was carried out as follows: 1 min at 94 °C, annealing for 1 min at 51 °C, and extension for 1.5 min at 72 °C, for 25 cycles, followed by extension for 5 min at 72 °C. The purified 1.6 kb PCR product was ligated into the pCR 2.1 TA cloning vector (Invitrogen) to produce TA-PCR. The clones with the correct insert size were sequenced to confirm the presence of the sequence specific for CYP4C7. Clones with the *Sst*I restriction site of the TA vector located downstream of the PCR product were used for further cloning.

A fragment of DNA of 240 bp between the *Afl*II and *Mun*I restriction sites contained the desired substitution and needed to be inserted into the wild-type P450BM3 gene. However, direct insertion of this fragment into pbsBM3 was unsuccessful, and thus, a different cloning protocol was used. The 1.6 kb fragment obtained after restriction of TA-PCR with *Afl*II and *Sst*I was cloned into the pbsBM3 expression vector that had been pretreated with the same restriction enzymes to produce the pBM3-C1 clone. This was treated with *Mun*I and *Sst*I enzymes, and the resulting 1.4 kb fragment was replaced with the 3.0 kb fragment from the wild-type pbsBM3 to produce the pBM3-4C7 protein expression vector.

Expression and Purification of the BM3−*4C7 Chimeric Enzymes.* Expression of the chimeric proteins was carried out under control of the P450BM3 natural promoter, as described for wild-type P450BM3 (*27*). Briefly, a 5 mL overnight culture was used to inoculate 500 mL of LB medium containing 50 μg/mL ampicillin, and cultures were incubated for 8 h at 37 °C at 200 rpm. The temperature was decreased to 30 °C, and the cultures were incubated for an additional 16 h at 150 rpm. The cells were harvested and washed with Tris-buffered saline. The cell pellets were pink, suggesting expression of the hemoprotein. A Western blot of the whole cells with anti-P450BM3 antibodies revealed expression of the full-size protein. The chimeric proteins were purified according to the protocol described for wild-type P450BM3 (*27*).

Activity Assays. Palmitate hydroxylation was carried out essentially as described previously (*10*). Briefly, 500 μL samples contained 100 μM NADPH, 250 μM palmitate, and an NADPH regenerating system consisting of 2 mM glucose 6-phosphate and 2 units/mL glucose-6-phosphate dehydrogenase in 0.1 M Tris-HCl buffer (pH 7.7). The reactions were started by enzyme addition, and the mixtures were incubated for 20−60 s with P450BM3 or for 2−10 min with the chimeric proteins. The reaction was stopped by the addition of 200 μL of 1.0 N HCl. Fatty acids and reaction products

were extracted with 2.5 mL of diethyl ether and methylated with diazomethane. Methyl esters were separated by GC-FID using a 12 m DB-1 capillary column (J&W). The reaction rate was calculated on the basis of the integrated peak areas of the product formed and substrate remaining.

A similar procedure was used to assess farnesol oxidation, except 100 μM farnesol was used and the incubation time was varied from 2 to 15 min. At the end of the incubation, 1.0 mL of the reaction mixture was applied on a 200 μg C18 solid-phase extraction column. The column was washed with 2 mL of water, and farnesol and reaction products were eluted with 1.0 mL of methanol. The eluate was directly analyzed by GC-FID as described above for palmitate hydroxylation.

Identification of Products of Oxidation of Farnesol and Palmitate. Synthesis of the reaction products for NMR analysis was carried out in 100−200 mL reaction mixtures containing 200 μM farnesol, 100 μM NADPH, 5 mM glucose 6-phosphate, 10 units of glucose-6-phosphate dehydrogenase, and 0.1−1.0 μM P450BM3 or one of the chimeric proteins. The reaction progress was monitored by GC-FID. When complete conversion of farnesol was achieved, nonpolar compounds were separated from the reaction mixture by solid-phase extraction using C18 solid-phase extraction columns (Burdick and Jackson). Before sample application, the columns were washed with methanol and water. After sample application, the columns were washed with water, and the reaction products were eluted with methanol. The eluates from several columns were pooled, dried under vacuum, and dissolved in deuterated methanol. (CD_3OD was chosen to avoid the presence of DCl, which might open epoxides, if $CDCl_3$ were used.) NMR spectra have been reported for some of the oxidation products, but only in other solvents (*28*, *29*). ^{1}H NMR spectra were recorded at 500 and 600 MHz on Bruker AVANCE DRX-500 and DRX-600 NMR spectrometers.

Essentially the same procedure was used for preparation of the products of palmitic acid oxidation for analysis by GC−MS. The reaction products and unreacted palmitic acid were isolated from the reaction mixture using C18 solid-phase extraction columns, and the MeOH eluate was dried under vacuum. The residue was dissolved in ethyl ether, and fatty acids were converted to methyl esters by treatment with diazomethane. The volatiles were removed by evaporation under a stream of nitrogen. The residue was dissolved in 100 μL of acetonitrile; 100 μL of bis(trimethylsilyl)-trifluoroacetamide was added for trimethylsilylation of hydroxyl groups, and the reaction was allowed to proceed overnight at 25 °C. The reaction mixture was directly analyzed by electron impact GC−MS using a Varian (Walnut Creek, CA) Saturn 2000 gas chromatograph−mass spectrometer system. The GC column was a Hewlett-Packard (Palo Alto, CA) HP-5ms with a length of 30 m, an internal diameter of 0.25 mm, and a film thickness of 0.33 μm. The temperature of the column oven was programmed as follows: initial temperature of 80 °C, hold for 1 min, increase at a rate of 20 °C/min to 300 °C, and hold for 8 min. The mass spectra were collected using electron ionization at 70 eV.

Other Procedures. Protein concentrations were determined by the Lowry procedure (*30*) using bovine serum albumin as a standard. The molar concentration of P450BM3 was calculated on the basis of the protein content using a molecular mass of 119 000 Da (*5*).

RESULTS AND DISCUSSION

Site of Chimeragenesis. CYP4C7 was shown to catalyze regio- and stereospecific hydroxylation of farnesol to produce (10*E*)-12-hydroxyfarnesol as a major product (*25*). As shown below, P450BM3 catalyzes oxidation of farnesol with formation of 9-hydroxyfarnesol and 2,3- and 10,11-epoxyfarnesols. The availability of the two enzymes that catalyze monooxygenation of farnesol to produce different products prompted us to develop and apply a new approach to altering the substrate specificity of P450BM3, scanning chimeragenesis. The structure of the BMP−palmitoleate complex (*24*) was used to determine which fragments of the protein are involved in substrate binding. Amino acids of BMP located within 7 Å of the bound fatty acid were mapped (Figure 1, bold residues). These are the fragments of the protein molecule that are likely to participate in substrate recognition and binding. Indeed, participation of some of these residues in substrate binding has been identified by site-directed mutagenesis (*12*−*17*).

Figure 1 also shows a sequence alignment of CYP4C7 and P450BM3 generated with the GAP program of the GCG package. Significant deviations in the N-terminal regions are explained by two factors. First, the 20−30 N-terminal amino acids of microsomal P450s form the membrane anchor, which is not present in P450BM3. Second, this region encompasses the first substrate recognition site (SRS) thought to determine the substrate specificity of cytochrome P450 enzymes (*31*), and is expected to vary significantly for enzymes with different substrate specificities.

Figure 2 shows five protein fragments that form the fatty acid binding site. In this study, we chose the fragment of P450BM3 corresponding to amino acids 73−84 to be replaced with amino acids 97−108 of CYP4C7. This fragment contributes to the formation of almost two-thirds of the length of the substrate binding channel. Figure 3 shows the four designed chimeric proteins, with 10 or fewer amino acids of P450BM3 replaced with the corresponding fragments of CYP4C7. The numbers in parentheses in the names of the chimeric proteins designate the replaced amino acid residues.

Expression and Purification of Chimeric Proteins. The four chimeric proteins as shown in Figure 3 were engineered, expressed, and characterized. The C(73−84), C(73−78), and C(75−80) enzymes were expressed at the same levels as wild-type P450BM3, yielding 250−300 nmol of purified protein/L of culture. The expression level of the C(78−82) enzyme was lower; the yield was in the range of 50−70 nmol/L of culture. A Western blot of the whole cell lysates with P450BM3-specific antibodies (data not shown) revealed expression of the full-size proteins. Ultrasonic cell disruption followed by ultracentrifugation to separate membrane and cytosolic fractions demonstrated that as in the case of the wild-type P450BM3, the chimeric proteins were expressed in the soluble form. Purification procedures similar to those described for wild-type P450BM3 (*27*) were successfully used to purify the chimeric proteins.

Spectral Properties of the BM3−4C7 Chimeric Enzymes. Wild-type P450BM3 and the chimeric proteins had es-

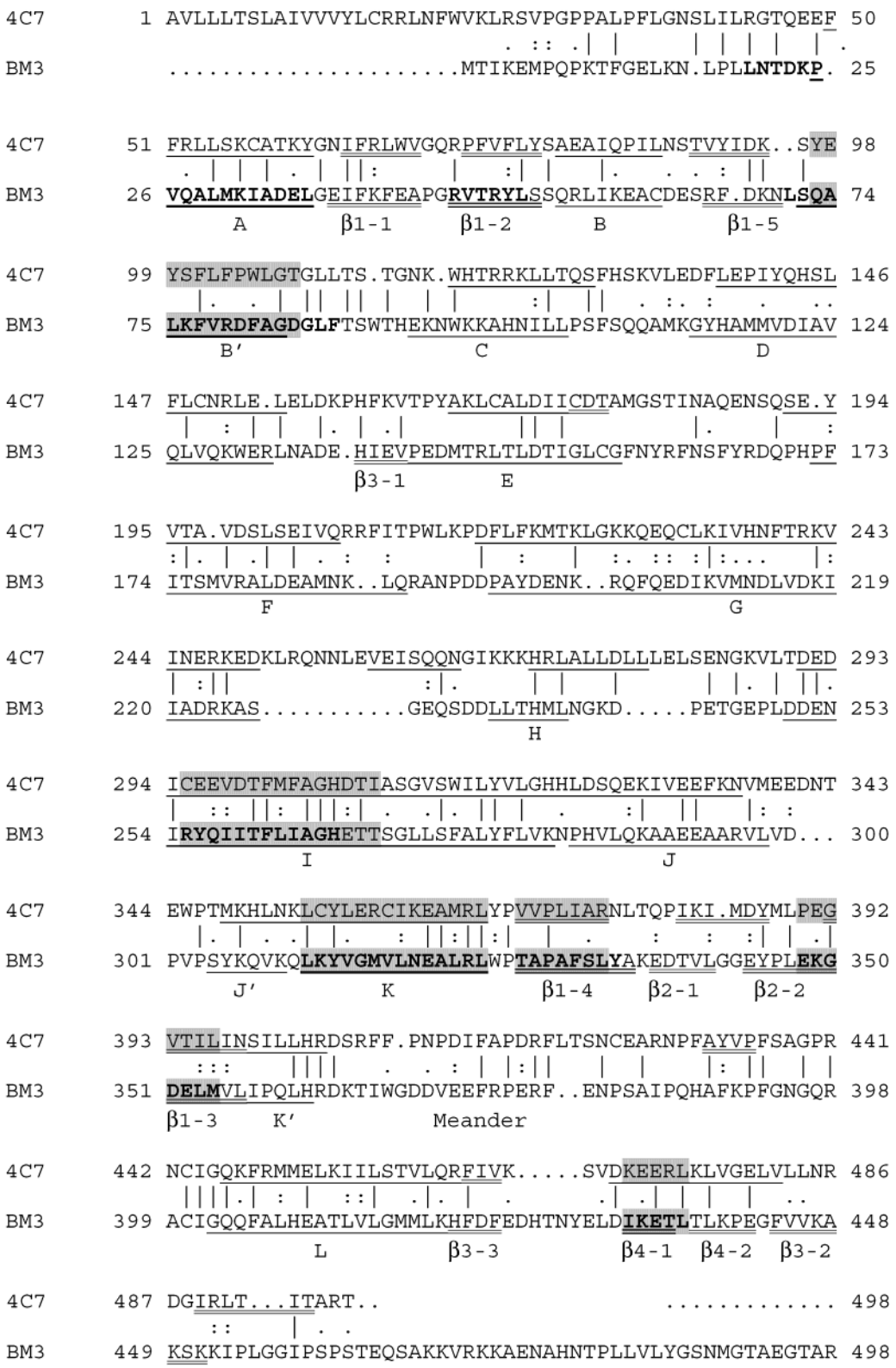

FIGURE 1: Sequence alignment of CYP4C7 and the heme domain of P450BM3. Residues mapped within 7 Å of the bound palmitate in the structure of Li and Poulos (*24*) are shown in bold. P450BM3 secondary structure elements are from ref *23*. α-Helices are underlined, and *β*-sheets are double underlined. The homologous fragments of the substrate binding site are shaded.

sentially identical absorbance spectra. Figure 4 shows absorbance spectra of P450BM3 and C(73−84), which harbored the largest substitution. Both proteins clearly had a Soret band indicative of the bound heme, and elevated absorbances at ∼350 and ∼470 nm indicative of the bound flavin cofactors. The spectra of C(73−78), C(75−80), and C(78−82) were practically identical to those shown in Figure 4 and are not presented. The results of these spectroscopic experiments suggest that the chimeric proteins fold properly and contain all the cofactors required for catalysis.

Because formation of the CO−ferrous adduct by P450BM3 occurs only when substrate is bound (*32*, *33*), these assays were carried out in the presence of 25 μM palmitate. Figure 5 shows difference spectra obtained with P450BM3 and the

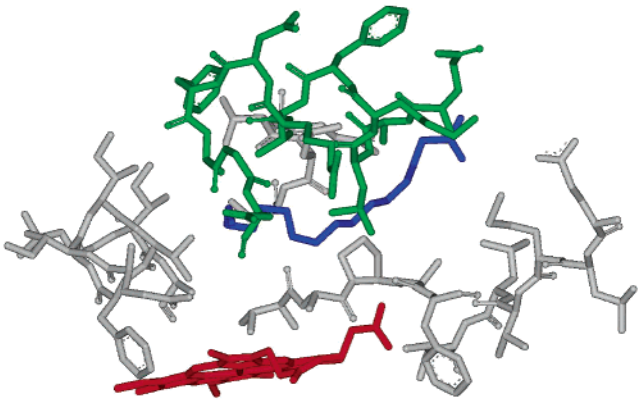

FIGURE 2: Protein fragments forming the substrate binding site of P450BM3. Heme and palmitoleic acid are colored red and blue, respectively. Residues 73−84 are colored green.

BM3	73	**Q**	**A**	**L**	**K**	**F**	**V**	**R**	**D**	**F**	**A**	**G**	**D** 84
C(73-84)		Y	E	Y	S	F	L	F	P	W	L	G	T
C(73-78)		Y	E	Y	S	F	L	R	D	F	A	G	D
C(75-80)		Q	A	Y	S	F	L	F	P	F	A	G	D
C(78-82)		Q	A	L	K	F	L	F	P	W	L	G	D

FIGURE 3: Replacements made in P450BM3 for chimeragenesis. P450BM3 amino acids 73−82 are shown. Shaded areas show the residues that have been replaced.

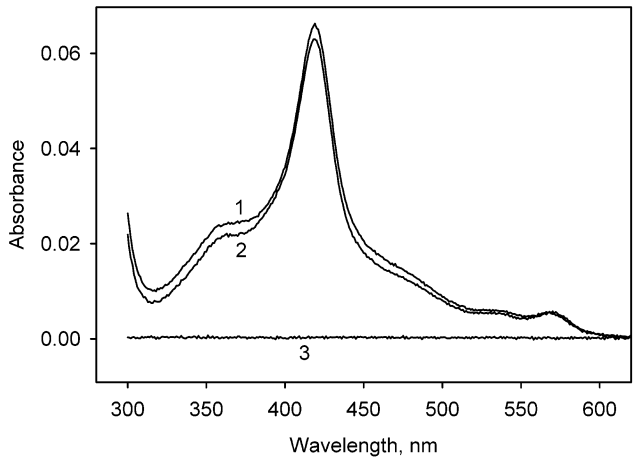

FIGURE 4: Absorbance spectra of 0.6 μM P450BM3 (spectrum 1) and 0.57 μM C(73−84) chimeric protein (spectrum 2). Spectrum 3 is the background spectrum.

chimeric proteins with NADPH as a reductant. C(73−84) showed no formation of the CO−ferrous adduct. C(73−78) and C(75−80) showed formation of the adduct with intensities that were ∼25−30% of that of the wild-type enzyme. The most active chimeric protein, C(78−82), showed formation of the CO complex with an intensity that was ∼70−75% of that of P450BM3. Only C(75−80) showed any formation of a P420 peak. None of the proteins showed any additional formation of the P450 complex or conversion to the P420 complex upon reduction by sodium dithionite before or after reduction by NADPH (not shown).

The purified chimeric enzymes did not show any increased protein instability compared to wild-type P450BM3. As shown by CO binding spectra, neither C(75−80), which

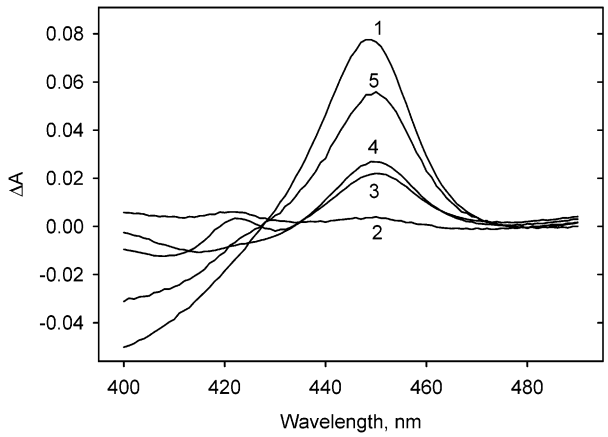

FIGURE 5: CO binding by P450BM3 and chimeric proteins. All enzymes were present at 1 μM: (1) P450BM3, (2) C(73−84), (3) C(73−78), (4) C(78−82), and (5) C(75−80). The reaction was carried out in a CO-saturated 0.1 M Tris-HCl, pH 7.7 buffer in the presence of 25 μM palmitate. The spectra were recorded 20 s after addition of 50 μM NADPH in the presence of the regenerating system.

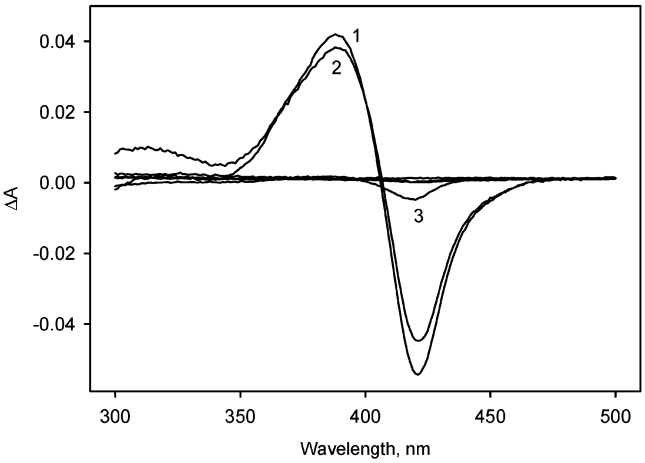

FIGURE 6: Type I spectral changes induced by 25 μM palmitate in P450BM3 (spectrum 1), C(78−82) (spectrum 2), and C(75−80) (spectrum 3). All enzymes were present at 1 μM. The reaction was carried out in 0.1 M Tris-HCl, pH 7.7 buffer. The spectra were recorded 20 s after addition of palmitate.

initially shows small amounts of a P420 form, nor the rest of the chimeric proteins show significant conversion of the P450 form to P420 over the course of incubation for 10 min at room temperature. These results indicate that despite the replacement of amino acids that can change the secondary structure of the protein, all the chimeras apparently fold properly.

Substrate Binding by the Chimeric Proteins. The small amplitude of the spectral changes indicating CO complex formation may be explained by impaired binding of palmitate by the chimeric proteins. The following experiments were carried out to characterize substrate binding.

It is well-established that palmitate induces type I spectral changes of the P450BM3 heme iron. This is shown in spectrum 1 of Figure 6. In contrast, chimeric proteins C(73−84) and C(73−78) produced very little if any type I spectral shift, so their difference spectra practically overlap the baseline. In contrast, C(78−82) showed a spectral shift typical for substrate binding by P450 enzymes upon palmitate

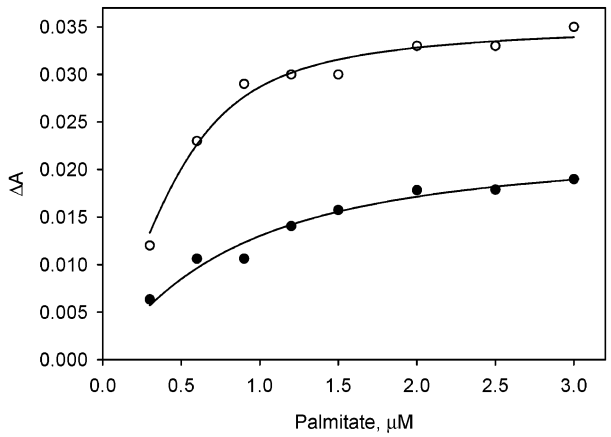

FIGURE 7: Palmitate binding by P450BM3 and C(78−82). The reaction was carried out in 0.1 M Tris-HCl, pH 7.7 buffer. Concentrations of the enzymes were 0.6 μM for P450BM3 (○) and 0.44 μM for C(78−82) (●), and the palmitate concentration was varied from 0.3 to 3.0 μM. The spectra were recorded 20 s after addition of palmitate.

addition (spectrum 2). C(75−80) also exhibited some spectral shift upon palmitate binding (spectrum 3), but with a maximal amplitude of only ~15% of that of P450BM3. The spectra shown in Figure 6 were obtained with 25 μM palmitate. Higher concentrations of palmitate did not increase the amplitude of the spectral shift, likely because of the low solubility of palmitate. These experiments clearly demonstrate that chimeragenesis alters palmitate binding, and lack of binding can explain the low yield of the CO complex by three of the chimeric proteins.

The affinities of P450BM3 and C(78−84), the only chimeric enzyme that exhibited a significant type I spectral shift upon palmitate binding, were measured spectrophotometrically. The amplitude of the spectral shift was plotted as a function of the added palmitate concentration (Figure 7). Because this assay requires relatively high protein concentrations, the binding curve was calculated using a mutually depleting model (*34*). The amplitude of the spectral change, $\Delta A_{390-424}$, was plotted as a function of the concentration of added palmitate, and the experimental curves were fitted to eq 1 for a single binding site and unknown maximal amplitude:

$$A = A_{max}\frac{[E]_t + [L]_t + K_d - \sqrt{([E]_t + [L]_t + K_d)^2 - 4[E]_t[L]_t}}{2[E]_t} \quad (1)$$

where A and A_{max} are the observed and maximal spectral change, respectively, $[E]_t$ and $[L]_t$ are the total concentrations of the enzyme and ligand, respectively, and K_d is the dissociation constant. The best fit to the above equation gave a K_d value of 0.16 ± 0.08 μM and an A_{max} of 0.058 ± 0.002 AU/μM. The following values were obtained for the C(78−82) enzyme: K_d = 0.55 ± 0.27 μM and A_{max} = 0.051 ± 0.004 AU/μM. The K_d value for P450BM3 appears to be somewhat lower than that of the C(78−82) enzyme. However, due to the large experimental error of these assays, which results in large standard deviations, the difference in the affinities of the two enzymes is not statistically significant.

Table 2: Catalytic Activities of P450BM3 and Chimeric Proteins

	cytochrome *c* reductase (s^{-1})	palmitate oxidation (min^{-1})	farnesol oxidation (min^{-1})
P450BM3	136 ± 2	3240 ± 420	344 ± 56
C(73−84)	130 ± 3	0.24 ± 0.06	26 ± 2
C(73−78)	158 ± 3	1.7 ± 0.3	29 ± 3
C(75−80)	270 ± 9	190 ± 15	5.3 ± 0.5
C(78−82)	140 ± 8	2643 ± 340	360 ± 5

Substrate binding experiments revealed that farnesol induced a small type I spectral shift in P450BM3 and the chimeric proteins. The amplitude for all the proteins was the same, reaching only ~10−15% of the amplitude induced by palmitate binding by wild-type P450BM3 (data not shown).

Catalytic Activities of the Chimeric Enzymes. To characterize the electron transfer function of the flavoprotein domain, cytochrome *c* reductase activities of the chimeric proteins were compared to that of wild-type P450BM3. The C(73−84), C(73−78), and C(78−82) chimeric proteins catalyzed reduction of cytochrome *c* with rates close to that of P450BM3 (Table 2). The activity of C(75−80) was elevated ~2-fold compared to those of the rest of the proteins. These measurements of cytochrome *c* reductase activity demonstrate that the flavoprotein domain of the chimeric proteins retains the ability to transfer electrons from NADPH to cytochrome *c*. This indicates that all the chimeric proteins have both flavin cofactors bound, as both FAD and FMN are required for cytochrome *c* reductase activity by P450BM3 (*35*).

Monooxygenase activities of the chimeric proteins were measured with palmitate and farnesol as substrates (Table 2). As more than one product was produced with both substrates, the activities shown in Table 2 represent the sum of all products made.

Replacement of amino acids 73−84 inhibited palmitate hydroxylase activity by 4 orders of magnitude. The chimeric protein in which residues 73−78 have been replaced inhibited palmitate hydroxylation by 3 orders of magnitude. In contrast, replacement of the second half of the fragment, amino acids 78−82, produced an enzyme with palmitate hydroxylase activity inhibited by only ~20%. Replacement of the six amino acids in the middle, residues 75−80, resulted in 17-fold inhibition of palmitate hydroxylase activity.

Replacement of residues 73−84 or 73−78 resulted in 12−13-fold inhibition of farnesol oxidation (Table 2). C(78−82) had unaltered farnesol oxidation compared to wild-type P450BM3. Somewhat surprisingly, replacement of 5 residues (75−80) inhibited farnesol oxidase activity to an even greater extent than replacement of 12 residues (73−84). Analysis of the monooxygenase activities of the chimeric proteins (Table 2) revealed that residues 73−78 were more critical for enzyme activity with both substrates tested than residues 78−82.

One of the striking findings is that palmitate and farnesol oxidations were inhibited to a different extent. For example, palmitate hydroxylation was inhibited by more than 4 orders of magnitude in C(73−84), while oxidation of farnesol was inhibited only 13-fold. Palmitate hydroxylation by C(73−78) was inhibited 1900 times, while only 12-fold inhibition

Table 3: Chemical Shifts (δ) and Coupling Constants (Hertz) in CD_3OD for Farnesol and Its Monooxygenation Products

atom	farnesol	2,3-epoxide	10,11-epoxide	9-hydroxyfarnesol	5-hydroxyfarnesol
1	4.01 d (6.5)	**3.52 dd (12.5, 6),**[a] **3.62 dd (12.5, 5)**		4.00 d (6.5)	3.98 dd (12.5, 6.5), 4.02 dd (12.5, 5)
2	5.28 t hex (6.5, 1.5)	**2.83 dd (6, 5)**	5.28 t hex (6.5, 1.5)	5.28 t hex (6.5, 1.5)	**5.33 t hex (6.5, 1.5)**
4	1.97 t (8)				1.94−2.07 m, 2.18 dd (13.5, 7.5)
5	2.05 q (8)				**4.41 ddd (8.5, 7, 6)**
6	5.06 t hex (6.5, 1.5)		5.12 t hex (6.5, 1.5)	5.10 t hex (6.5, 1.5)	5.08 d hex (8.5, 1.5)
8	1.90 t (8)			1.95−2.08 m, 2.15 dd (13.5, 7.5)	1.94 t (8)
9	2.00 q (8)			**4.35 dt (8.5, 7)**	1.94−2.07 m
10	5.02 t hep (6, 1.5)		2.68 t (6.5)	**5.04 d hep (8.5, 1.5)**	5.02 t hep (6, 1.5)
12	1.59 br s		**1.21 s**[b]	1.59 d (1.5)	1.60 br s
13	1.59 br s	1.20 s		1.60 br s	1.63 br s
14	1.52 br s			1.59 br s	1.60 br s
15	1.53 br s		**1.18 s**[b]	1.64 d (1.5)	1.53 br s

[a] Resonances unique to each compound are in bold. [b] May be reversed.

of farnesol oxidation was detected. On the other hand, C(75−80) inhibited farnesol oxidation 65-fold, while palmitate hydroxylation was inhibited by a factor of only 17. The most active chimeric protein, C(78−82), inhibited palmitate hydroxylation by ∼20% with no effect on the oxidation of farnesol.

The lack of a correlation of the extent of inhibition of the activities with two substrates also followed from the comparison of C(73−84) and C(75−80). The shortening of the insert increased palmitate hydroxylase activity by 3 orders of magnitude, while farnesol oxidation was inhibited further by a factor of 5.

These findings indicate that some functional groups of the enzyme catalytic site may be involved to a different extent in the binding and/or catalytic conversion of the different, although homologous, substrates, even if the same chemical conversion occurs. This idea is supported by the finding that mutation of E267 altered the regiospecificity of fatty acid hydroxylation by P450BM3, but with a greater effect on hydroxylation of palmitate than laurate (*16*). These observations suggest that different catalytic steps, different rate-limiting steps, or even different mechanisms are utilized by one enzyme for oxidation of different substrates.

Farnesol Metabolism and Product Identification. Incubation of P450BM3 in the presence of farnesol resulted in two major peaks with retention times of 17.9 and 19.7 min as detected by GC-FID, as shown in Figure S2 of the Supporting Information. The two major peaks observed with wild-type P450BM3 were still produced by the chimeric proteins, but an additional peak with a retention time of 20.0 min appeared for three of the four chimeric proteins, indicating formation of a new product. To identify the products of farnesol oxidation, the reaction products were analyzed by ^{1}H NMR spectroscopy.

The spectral assignments for the products are given in Table 3. From these assignments, it is concluded that wild-type P450BM3 catalyzes formation of farnesol 2,3-epoxide, farnesol 10,11-epoxide, and 9-hydroxyfarnesol. In addition to these compounds, the C(73−84), C(73−78), and C(75−80) chimeric proteins catalyzed formation of 5-hydroxyfarnesol. 9-Hydroxyfarnesol and 5-hydroxyfarnesol have retention times of 19.7 and 20.0 min, respectively (Figure S2 of the Supporting Information). Analysis of the oxidation products from the chimeric proteins revealed that the two epoxides are not separated under the GC-FID conditions used and had a retention time of 17.9 min. Farnesol 6,7-epoxide may have also been present, but in such small amounts that we could not distinguish its peaks from small peaks possibly arising from doubly oxidized products. The resonance assignments were made as follows.

The most definitive peaks for 9-hydroxyfarnesol were at δ 4.35 for H9 and δ 5.04 for H10, which showed that the new hydroxyl group was secondary and coupled to a vinyl hydrogen; since the latter resonance was a doublet of heptets, the vinyl hydrogen had to be H10 and not H6. NMR analysis of the C(73−78) products indicated another secondary alcohol with peaks reminiscent of those of 9-hydroxyfarnesol, but with the multiplet for the vinyl hydrogen occurring at δ 5.08 and showing a doublet−hextet pattern consistent with only 5-hydroxyfarnesol. The H1 protons were now nonequivalent due to the nearby chiral center. 5-Hydroxyfarnesol is a new compound.

Methyl resonances between δ 1.18 and 1.21 and methinyl resonances at δ 2.68 and 2.83 indicated that the other major components were epoxides. With wild-type P450BM3, the more abundant one had to be the 10,11-epoxide because it had *two* upfield methyl resonances (δ 1.18 and 1.21), while the minor one was the 2,3-epoxide because its H1 proton resonances were shifted well upfield and were now nonequivalent (δ 3.52 and 3.62). Table 3 summarizes chemical shifts of farnesol and products of its oxidation. The absolute configurations of the oxidation products were not determined in this study, but are the subject of future research.

Palmitate Metabolism and Product Identification. Palmitate hydroxylation by the chimeric proteins produced multiple products, as shown by the GC-FID traces shown in Figure S3 of the Supporting Information. The products of palmitate hydroxylation by wild-type P450BM3 and the chimeric proteins were identified by GC−MS of the TMS derivatives of the methyl esters (*36*). As chimeragenesis altered palmitate hydroxylation activity, with both turnover numbers and products formed being affected, GC−MS analysis of the reaction products was carried out (Figure S4 of the Supporting Information). The activities of C(73−84) and C(73−78) with palmitate as the substrate were inhibited by 4 and 3 orders of magnitude, respectively (Table 2). The replacements that produced C(75−80) and C(78−82) had modest effects on palmitate hydroxylation (Table 2), so sufficient

Table 4: Unique MS Ions Used for Identification of Palmitate Metabolites[a]

	ion A	ion B	ion C		ion A	ion B	ion C
15-OH	117	343	314	12-OH	159	301	272
14-OH	131	329	300	11-OH	173	287	258
13-OH	145	315	286	10-OH	187	273	244

[a] Ion A, proximal α cleavage; ion B, distal α cleavage; ion C, migration of TMS to a carbomethoxy group along with proximal α cleavage.

amounts of the TMS derivatives of the methyl esters of the reaction products could be obtained for identification by GC−MS.

Two groups of ions were used to identify reaction products. The first group was common to all of the hydroxylated palmitic acid derivatives: *m*/*z* 343 ($[M - CH_3]^+$), 327 ($[M - CH_3O]^+$), 311 ($[M - CH_3 - CH_3OH]^+$), and 73 $\{[(CH_3)_3Si]^+\}$ (as shown in Figure S4 of the Supporting Information). The second group (Table 4) consisted of fragmentation peaks differing by 14 mass units (CH_2) which showed the position of hydroxylation: the series from *m*/*z* 117 to 187 $\{[CH_3(CH_2)_nCHOTMS]^+\}$, the series from *m*/*z* 343 to 273 $\{[TMSOCH(CH_2)_nCOOCH_3]^+\}$, and the series from *m*/*z* 314 to 244 $\{[TMS(CH_2)_nCOOCH_3]^+\}$. The fragmentation pattern found here is consistent with the mass spectra of TMS derivatives of methyl esters of hydroxylated palmitic acids published previously (*37*).

The products of palmitate hydroxylation by wild-type P450BM3 were identified as 15-, 14-, and 13-OH, corresponding to ω-1, ω-2, and ω-3 hydroxylation, respectively, in agreement with previous studies (*38*−*40*). The chimeric enzymes produce these same reaction products, but also products with shorter retention times. The additional products formed by C(78−82) and C(75−80) were identified by GC−MS as 12-, 11-, and 10-OH, with the latter having the shortest retention time. Formation of small amounts of 11- and 12-hydroxypalmitate by P450BM3 has been reported (*36*), while formation of 10-hydroxypalmitate is a new activity. Because of the very low palmitate hydroxylase activity of C(73−84) and C(73−78), their regiospecificity of hydroxylation was not analyzed by GC−MS. However, on the basis of the retention times of the products (Figure S4 of the Supporting Information), C(73−84) and C(73−78) also produced 12-, 11-, and 10-hydroxypalmitates in addition to the three products formed by the wild-type enzyme.

Regiospecificity of Farnesol and Palmitate Monooxygenation. The results shown in Table 2 demonstrate that, with the exception of C(78−82), the replacement of amino acids made within the region of residues 73−84 produced variant enzymes with both palmitate hydroxylation and farnesol oxidation inhibited as compared to the reactions for the wild-type enzyme. These changes in specific activity were accompanied by alteration of the regiospecificity of oxygenation, as demonstrated by product identification.

Table 5 presents the ratios of the products formed by P450BM3 and the chimeric proteins with farnesol as a substrate. Because different isomers of farnesol epoxide were not separated by GC-FID, all the epoxides were treated as a single product, although the regiospecificity of epoxidation was altered by chimeragenesis (see below). In addition to epoxides and 9-hydroxyfarnesol formed by P450BM3, three of the chimeras, C(73−84), C(73−78), and C(75−80), produced a third product, 5-hydroxyfarnesol, which in the cases of C(73−78) and C(75−80) became a major product. Interestingly, replacement of amino acids 78−82 produces another enzyme that catalyzes hydroxylation at only one position with formation of 9-hydroxyfarnesol.

Table 5: Ratios of Product Formation during Farnesol Oxidation by P450BM3 and the Chimeric Proteins[a]

	epoxides	9-OH	5-OH
P450BM3	1	0.89 ± 0.01	ND[b]
C(73−84)	1	1.03 ± 0.06	0.67 ± 0.03
C(73−78)	1	0.34 ± 0.02	1.75 ± 0.04
C(75−80)	1	1.03 ± 0.04	1.61 ± 0.04
C(78−82)	1	1.01 ± 0.11	ND[b]

[a] The epoxide peak was taken to be the standard. The numbers are the average of six measurements with standard deviations given. [b] Not detected.

Comparison of peak intensities in NMR spectra revealed that the regiospecificity of epoxidation is also changed by chimeragenesis. P450BM3 forms 10,11-epoxyfarnesol and 2,3-epoxyfarnesol in a ratio of 3:2. C(73−84) and C(73−78) still catalyze formation of 10,11-epoxyfarnesol but produce only traces of 2,3-epoxyfarnesol, while no detectable formation of 2,3-epoxyfarnesol was observed for C(78−82). Thus, C(73−78) (residues 73−78) and C(78−82) (residues 78−82) have the same regiospecificity in farnesol epoxidation, but different preferences in the hydroxylation reaction.

No significant amounts of double oxidation products were detected, even when almost complete oxidation of farnesol was achieved when the samples for NMR analysis were prepared. This indicates that the initial products of farnesol oxidation did not undergo secondary oxygenation at significant rates.

C(75−80) had very little farnesol monooxygenase activity, and no attempt was made to isolate and identify the reaction products by NMR. However, the GC-FID profile (Figure 3S of the Supporting Information) suggests formation of epoxide(s), 5-hydroxyfarnesol and 9-hydroxyfarnesol.

The regiospecificity of palmitate hydroxylation was also changed by chimeragenesis (Table 6). P450BM3 catalyzed hydroxylation of C13−C15 of palmitic acid; minute quantities of products hydroxylated at the 11 and 12 positions were also detected, in agreement with a previous report (*36*). All of the chimeric proteins catalyze formation of 10-, 11-, and 12-hydroxypalmitates. C(78−82) and C(75−80), the most active chimeric proteins with palmitate as the substrate, catalyze the formation of significant amounts of 11- and 12-hydroxypalmitates, as well as formation of 10-hydroxypalmitate (Table 6). In the case of C(75−80) and C(78−82), 10-hydroxypalmitate was formed in significant quantities, while the enzymes retained significant catalytic activity. Products of the more active C(78−82) and C(75−80) proteins were identified by GC−MS, while product assignments for C(73−84) and C(73−78) were based on GC-FID retention times because of their low activity. Formation of 10-hydroxypalmitate by wild-type or mutant P450BM3 has not been reported previously.

Table 6 also shows the rates of formation of the regioisomers of hydroxypalmitates calculated on the basis of the overall rate of palmitate hydroxylation (Table 2) and product distribution. Analysis of the reaction rates revealed that in the case of C(77−82) the rates of formation of 11- and 12-

Table 6: Ratios and Rates of Product Formation during Palmitate Oxidation by P450BM3 and the Chimeric Proteins[a]

protein	10-OH	11-OH	12-OH	13-OH	14-OH	15-OH
P450BM3	ND[b] (0)	0.017 ± 0.005 (16)	0.040 ± 0.005 (32)	0.89 ± 0.1 (810)	1.56 ± 0.05 (1426)	1 (940)
C(73−84)	1.30 ± 0.56 (0.05)	0.57 ± 0.3 (0.02)	0.67 ± 0.15 (0.02)	2.15 ± 0.33 (0.02)	1.31 ± 0.15 (0.05)	1 (0.03)
C(73−78)	1.76 ± 0.09 (0.46)	0.63 ± 0.02 (0.17)	0.43 ± 0.04 (0.12)	1.41 ± 0.02 (0.36)	1.35 ± 0.04 (0.36)	1 (0.26)
C(75−80)	0.81 ± 0.07 (19)	1.53 ± 0.09 (34)	0.77 ± 0.15 (17)	2.43 ± 0.15 (55)	1.96 ± 0.05 (44)	1 (23)
C(78−82)	0.21 ± 0.05 (106)	0.21 ± 0.03 (106)	0.37 ± 0.02 (212)	1.62 ± 0.06 (872)	1.52 ± 0.08 (819)	1 (529)

[a] The 15-hydroxypalmitate peak is taken to be the standard. The numbers are the average of six measurements with standard deviations given. Rates of individual product formation during palmitate oxidation by P450BM3 and the chimeric proteins are shown in parentheses (min^{-1}). [b] Not detected.

hydroxypalmitates increase severalfold compared to those of wild-type P450BM3, while formation of 10-hydroxypalmitate is not catalyzed by P450BM3. C(75−80), although inhibited, catalyzes hydroxylation of six positions (C10−C15) with comparable rates. In the case of the chimeric proteins with very low activity [C(73−84) and C(73−78)], one can argue that the relative increase in the level of formation of 10-, 11-, and 12-hydroxypalmitates is caused by the dramatic inhibition of the wild-type activities toward C13−C15. However, the much more active C(75−80), and especially C(78−82), which is almost as active as wild-type P450BM3, also produce significant amounts of 10-OH, 11-OH, and 12-OH palmitates. In the case of C(78−82), the rates of formation of 11- and 12-hydroxypalmitates increased 7-fold compared to that of P450BM3 to 106 and 212 min^{-1}, respectively, while the rate of 10-hydroxypalmitate synthesis increased from 0 to 106 min^{-1}. Thus, at least in the case of C(78−82), chimeragenesis resulted in increased rates of formation of 10-OH, 11-OH, and 12-OH.

Concluding Remarks. Our approach produced four fully functional chimeric proteins with altered substrate binding properties and/or catalytic specificity. The fragment chosen for this study, amino acid residues 73−84 of P450BM3, is involved in substrate binding, substrate specificity, and regiospecificity of catalysis. Introduction of protein fragments of CYP4C7 into the substrate binding pocket of P450BM3 resulted in the formation of enzymes capable of synthesis of new products, 10-hydroxypalmitate and 5-hydroxyfarnesol, compounds not formed by the wild-type enzyme. The major product of farnesol oxidation by the C(73−78) chimeric protein, 5-hydroxyfarnesol, is a compound that has not been synthesized before. In the case of palmitate, much larger amounts of 11- and 12-hydroxypalmitates are produced with the chimeric enzymes than the traces found with P450BM3 itself, and in contrast to P450BM3, the chimeric proteins catalyze formation of 10-hydroxypalmitate. These facts demonstrate the potential of the new approach, scanning chimeragenesis, in altering the substrate specificity of P450BM3 and in producing new compounds for potential biotechnological use.

It is noteworthy that position 5 is near the center of farnesol, and oxidation there requires that farnesol be able to enter the cavity more deeply. This happens most with C(73−78), the enzyme which produces 5-hydroxyfarnesol and 10-hydroxypalmitate as major products. It seems likely that the modifications in C(73−78) permit the nonpolar ends of the farnesol and palmitate to penetrate further into the catalytic site, favoring oxidation at these interior positions. These deeper insertions may be largely due to the V78L mutation, the only change common to all four chimeric enzymes.

An F87A genetically engineered variant of P450BM3 revealed a new catalytic activity, hydroxylation of the terminal carbon atom in laurate (*14*). This reaction was not catalyzed by the wild-type enzyme. Here we report engineering enzyme variants with the regiospecificity of fatty acid hydroxylation shifted toward the center of the molecule. C(78−82) and C(75−80) catalyze palmitate hydroxylation at the ω-4, ω-5, and ω-6 positions. Thus, the two approaches, one published by Oliver and co-workers (*14*) and the second presented here, provide a means of shifting the regiospecificity of fatty acid hydroxylation to the terminal carbon or toward the center of the molecule.

ACKNOWLEDGMENT

We thank Professor Armand Fulco of the University of California (Los Angeles, CA) for a generous gift of the P450BM3 expression plasmid. This paper was revised when F.A.W. was on sabbatical leave at the Institute of Physics at the University of Lübeck (Lübeck, Germany) with support from an Alexander von Humboldt Senior Research Award.

SUPPORTING INFORMATION AVAILABLE

Cloning scheme for engineering a chimeric protein, CG-FID profiles of the products of oxidation of farnesol and palmitic acid by P450BM3 and chimeric proteins, and mass spectra of the products of palmitate hydroxylation by P450BM3 and chimeric proteins. This material is available free of charge via the Internet at http://pubs.acs.org.

REFERENCES

1. Nelson, D. R., Koymans, L., Kamataki, T., Stegeman, J. J., Feyereisen, R., Waxman, D. J., Waterman, M. R., Gotoh, O., Coon, M. J., Estabrook, R. W., Gunsalus, I. C., and Nebert, D. W. (1996) P450 superfamily: update on new sequences, gene mapping, accession numbers and nomenclature, *Pharmacogenetics 6*, 1−42.
2. Guengerich, F. P., and MacDonald, T. L. (1990) Mechanisms of cytochrome P-450 catalysis, *FASEB J. 4*, 2453−2459.
3. Guengerich, F. P., and Shimada, T. (1991) Oxidation of toxic and carcinogenic chemicals by human cytochrome P-450 enzymes, *Chem. Res. Toxicol. 4*, 391−407.
4. Guengerich, F. P. (1995) Cytochrome P450 proteins and potential utilization in biodegradation, *Environ. Health Perspect. 103* (Suppl. 5), 25−28.
5. Narhi, L. O., and Fulco, A. J. (1986) Characterization of a catalytically self-sufficient 119,000-dalton cytochrome P-450 monooxygenase induced by barbiturates in *Bacillus megaterium*, *J. Biol. Chem. 261*, 7160−7169.
6. Fulco, A. J. (1991) P450BM-3 and other inducible bacterial P450 cytochromes: biochemistry and regulation, *Annu. Rev. Pharmacol. Toxicol. 31*, 177−203.
7. Munro, A. W., Leys, D. G., McLean, K. J., Marshall, K. R., Ost, T. W., Daff, S., Miles, C. S., Chapman, S. K., Lysek, D. A., Moser,

C. C., Page, C. C., and Dutton, P. L. (2002) P450 BM3: the very model of a modern flavocytochrome, *Trends Biochem. Sci. 27*, 250−257.
8. Matson, R. S., Hare, R. S., and Fulco, A. J. (1977) Characteristics of a cytochrome P-450-dependent fatty acid ω-2 hydroxylase from *Bacillus megaterium*, *Biochim. Biophys. Acta 487*, 487−494.
9. Boddupalli, S. S., Estabrook, R. W., and Peterson, J. A. (1990) Fatty acid monooxygenation by cytochrome P-450BM-3, *J. Biol. Chem. 265*, 4233−4239.
10. Murataliev, M. B., Klein, M., Fulco, A., and Feyereisen, R. (1997) Functional interactions in cytochrome P450BM3: flavin semiquinone intermediates, role of NADP(H), and mechanism of electron transfer by the flavoprotein domain, *Biochemistry 36*, 8401−8412.
11. Miles, C. S., Ost, T. W., Noble, M. A., Munro, A. W., and Chapman, S. K. (2000) Protein engineering of cytochromes P-450, *Biochim. Biophys. Acta 1543*, 383−407.
12. Graham-Lorence, S., Truan, G., Peterson, J. A., Falck, J. R., Wei, S., Helvig, C., and Capdevila, J. H. (1997) An active site substitution, F87V, converts cytochrome P450 BM-3 into a regio- and stereoselective (14S,15R)-arachidonic acid epoxygenase, *J. Biol. Chem. 272*, 1127−1135.
13. Oliver, C. F., Modi, S., Primrose, W. U., Lian, L.-Y., and Roberts, G. C. K. (1997) Engineering the substrate specificity of Bacillus megaterium cytochrome P-450 BM3: hydroxylation of alkyl trimethylammonium compounds, *Biochem. J. 327*, 537−544.
14. Oliver, C. F., Modi, S., Sutcliffe, M. J., Primrose, W. U., Lian, L. Y., and Roberts, G. C. (1997) A single mutation in cytochrome P450 BM3 changes substrate orientation in a catalytic intermediate and the regiospecificity of hydroxylation, *Biochemistry 36*, 1567−1572.
15. Noble, M. A., Miles, C. S., Chapman, S. K., Lysek, D. A., MacKay, A. C., Reid, G. A., Hanzlik, R. P., and Munro, A. W. (1999) Roles of key active-site residues in flavocytochrome P450 BM3, *Biochem. J. 339*, 371−379.
16. Yeom, H., and Sligar, S. G. (1997) Oxygen activation by cytochrome P450BM3: effect of mutating an active site acidic residue, *Arch. Biochem. Biophys. 337*, 209−216.
17. Cowart, L. A., Falck, J. R., and Capdevila, J. H. (2001) Structural determinants of active site binding affinity and metabolism by cytochrome P450 BM-3, *Arch. Biochem. Biophys. 387*, 117−124.
18. Li, Q. S., Schwaneberg, U., Fischer, P., and Schmid, R. D. (2000) Directed evolution of the fatty-acid hydroxylase P450 BM-3 into an indole-hydroxylating catalyst, *Chem.—Eur. J. 6*, 1531−1536.
19. Li, Q. S., Schwaneberg, U., Fischer, M., Schmitt, J., Pleiss, J., Lutz-Wahl, S., and Schmid, R. D. (2001) Rational evolution of a medium chain-specific cytochrome P-450 BM-3 variant, *Biochim. Biophys. Acta 1545*, 114−121.
20. Li, Q. S., Ogawa, J., Schmid, R. D., and Shimizu, S. (2001) Engineering cytochrome P450 BM-3 for oxidation of polycyclic aromatic hydrocarbons, *Appl. Environ. Microbiol. 67*, 5735−5739.
21. Appel, D., Lutz-Wahl, S., Fischer, P., Schwaneberg, U., and Schmid, R. D. (2001) A P450 BM-3 mutant hydroxylates alkanes, cycloalkanes, arenes and heteroarenes, *J. Biotechnol. 88*, 167−171.
22. Gilardi, G., Meharenna, Y. T., Tsothou, G. E., Sadeghi, S. J., Fairhead, M., and Giannini, S. (2002) Molecular Lego: design of molecular assemblies of P450 enzymes for nanotechnology, *Biosens. Bioelectron. 17*, 133−145.
23. Ravichandran, K. G., Boddupalli, S. S., Hasermann, C. A., Peterson, J. A., and Deisenhofer, J. (1993) Crystal structure of hemoprotein domain of P450BM-3, a prototype for microsomal P450's, *Science 261*, 731−736.
24. Li, H., and Poulos, T. L. (1997) The structure of the cytochrome p450BM-3 haem domain complexed with the fatty acid substrate, palmitoleic acid, *Nat. Struct. Biol. 4*, 140−146.
25. Sutherland, T. D., Unnithan, G. C., Andersen, J. F., Evans, P. H., Murataliev, M. B., Szabo, L. Z., Mash, E. A., Bowers, W. S., and Feyereisen, R. (1998) A cytochrome P450 terpenoid hydroxylase linked to the suppression of insect juvenile hormone synthesis, *Proc. Natl. Acad. Sci. U.S.A. 95*, 12884−12889.
26. Wen, L. P., and Fulco, A. J. (1987) Cloning of the gene encoding a catalytically self-sufficient cytochrome P-450 fatty acid monooxygenase induced by barbiturates in Bacillus megaterium and its functional expression and regulation in heterologous (*Escherichia coli*) and homologous (*Bacillus megaterium*) hosts, *J. Biol. Chem. 262*, 6676−6682.
27. Murataliev, M. B., and Feyereisen, R. (1996) Functional interactions in cytochrome P450BM3. Fatty acid substrate binding alters electron-transfer properties of the flavoprotein domain, *Biochemistry 35*, 15029−15037.
28. Mordini, A., Pecchi, S., Capozzi, G., Capperucci, A., Degl'Innocenti, A., Reginato, G., and Ricci, A. (1994) Heteroatom-Assisted Isomerization of Oxiranes to Allylic Alcohols Promoted by Bases, *J. Org. Chem. 59*, 4784−4790.
29. Zheng, Y. F., Oehlschlager, A. C., and Hartman, P. G. (1994) Synthesis of (6E)-8-Thia- and (14E)-13-Thia-2,3-oxidosqualene: Inhibitors of 2,3-Oxidosqualene-Lanosterol Cyclase, *J. Org. Chem. 59*, 5803−5809.
30. Lowry, O. H., Rosebrough, N. J., Farr, A. L., and Randall, R. J. (1951) Protein measurement with the Folin phenol reagent, *J. Biol. Chem. 195*, 265−275.
31. Gotoh, O. (1992) Substrate recognition sites in cytochrome P450 family 2 (CYP2) proteins inferred from comparative analyses of amino acid and coding nucleotide sequences, *J. Biol. Chem. 267*, 83−90.
32. Li, H. Y., Darwish, K., and Poulos, T. L. (1991) Characterization of recombinant *Bacillus megaterium* cytochrome P-450 BM-3 and its two functional domains, *J. Biol. Chem. 266*, 11909−11914.
33. Klein, M. L., and Fulco, A. J. (1994) The interaction of cytochrome *c* and the heme domain of cytochrome P-450BM-3 with the reductase domain of cytochrome P-450BM-3, *Biochim. Biophys. Acta 1201*, 245−250.
34. Segel, I. H. (1975) *Enzyme kinetics: behavior and analysis of rapid equilibrium and steady state enzyme systems*, Wiley-Interscience, New York.
35. Klein, M. L., and Fulco, A. J. (1993) Critical residues involved in FMN binding and catalytic activity in cytochrome P450BM-3, *J. Biol. Chem. 268*, 7553−7561.
36. Truan, G., Komandla, M. R., Falck, J. R., and Peterson, J. A. (1999) P450BM-3: absolute configuration of the primary metabolites of palmitic acid, *Arch. Biochem. Biophys. 366*, 192−198.
37. Nicolaides, N., Soukup, V. G., and Ruth, E. C. (1983) Mass spectrometric fragmentation patterns of the acetoxy and trimethylsilyl derivatives of all the positional isomers of the methyl hydroxypalmitates, *Biomed. Mass Spectrom. 10*, 441−449.
38. Miura, Y., and Fulco, A. J. (1974) (ω-2)Hydroxylation fo fatty acids by a soluble system from *Bacillus megaterium*, *J. Biol. Chem. 249*, 1880−1888.
39. Miura, Y., and Fulco, A. J. (1975) ω-1, ω-2 and ω-3 hydroxylation of long-chain fatty acids, amides and alcohols by a soluble enzyme system from *Bacillus megaterium*, *Biochim. Biophys. Acta 388*, 305−317.
40. Boddupalli, S. S., Pramanik, B. C., Slaughter, C. A., Estabrook, R. W., and Peterson, J. A. (1992) Fatty acid monooxygenation by P450BM-3: product identification and proposed mechanisms for the sequential hydroxylation reactions, *Arch. Biochem. Biophys. 292*, 20−28.

BI035674B